Electrical Power and Energy Systems 104 (2019) 549–561

Contents lists available at ScienceDirect

Electrical Power and Energy Systems

journal homepage: www.elsevier.com/locate/ijepes

Cost savings and emission reduction capability of wind-integrated power systems

Rajat Kanti Samal*, M. Tripathy

Department of Electrical Engineering, Veer Surendra Sai University of Technology Burla, Odisha 768018, India

ARTICLE INFO

Keywords:
Cost savings
Emission reduction
Emission factor
Turbine performance index
Economic emission dispatch

ABSTRACT

In the face of energy crisis and environmental impacts of conventional energy sources, renewable energy sources have attracted tremendous interest. Among many resources, wind energy has proven to be a promising renewable energy option in recent times. The primary objective of utilizing renewable energy is its environmental sustainability and the idea of emission reduction constitutes a prominent part in it. The emission here refers to the CO_2, SO_2 and NO_x emissions from thermal power plants. However, recent research works suggest that there remains a considerable anomaly between the claims of emission reduction by wind energy developers and the actual emissions, particularly with the integration of wind power into the grid system. The estimation methodology involving tools like wind resource assessment and energy capture may not provide accurate estimates due to some power system generation and operational constraints. The objective of the present study is to analyse the impact of wind turbine ratings and economic emission dispatch (EED) on the generation cost and emissions in wind integrated power systems. In this regard, the study investigates the concept of emission factor and wind-integrated EED. Wind turbines available at different rated power and rated speeds are incorporated in four different test power systems and the actual cost and emissions over a selected period are evaluated. Finally, the impact of the wind power integration on the generation cost savings and emission reduction is investigated.

1. Introduction

Environmental sustainability is one of the major components of the United Nations Millennium Development Goals (MDG) [1] in which the contribution of sustainable energy sources is important. The Clean Development Mechanism (CDM) of the Kyoto Protocol incorporated the principles of sustainable development and identified emission reduction as one of the primary components of sustainable energy [2]. The core of the CDM process lies in calculation of emission reduction and additionality for any project which aspires to obtain funds from CDM. Additionality signifies that the project should lead to real, measurable and long term greenhouse gas (GHG) reduction which are to be measured with reference to a baseline. For demonstrating emission reduction, ACM0002 and AMS I.D. methodologies respectively can be used for large scale and small scale grid connected renewable energy projects [3]. Wind is one of the fastest growing sustainable energy sources which have been considered by policy makers for meeting emission reduction targets. To evaluate the sustainability of a wind energy project, the amount of emission reduction over the lifetime of a project must be estimated. In CDM wind energy projects, grid emission factors have been used to determine the amount of emission reduction for claiming emission reduction benefits [4]. However, the estimated value of emission reduction may be inaccurate and may differ considerably from the actual value after integration of wind energy system to the grid. The reason may be attributed to the operational constraints associated with power system operation [5]. There have been attempts at quantification of emission reduction from wind generation based on correlation factor between time evolution of marginal emissions and wind generation [6]. Instead of considering only emission aspect, policy makers may carry out a thorough analysis related to the impact of large scale wind integration on power system operation and emission targets thereof.

In recent years, the issue of emission control from thermal generators has been incorporated into economic dispatch model resulting in a multiobjective optimization problem referred to as economic emission dispatch (EED) [7–9]. The research efforts towards obtaining efficient and robust stochastic algorithms for EED are still continuing [10–14]. In one recent approach, exchange market algorithm is used and cost and emission are obtained for IEEE 30 bus system including operational aspects [15]. In addition, deterministic mathematical programming based approaches have also been attempted [16]. In [17], multi-objective EED (MOEED) is implemented over a 24 h dispatch

* Corresponding author.
E-mail address: rajatksamal82@gmail.com (R.K. Samal).

https://doi.org/10.1016/j.ijepes.2018.07.039
Received 20 May 2017; Received in revised form 16 July 2018; Accepted 18 July 2018
Available online 26 July 2018

period and fuel cost and emission are calculated with different DSM participation levels and it is concluded that emission reduction takes place with more participation of DSM. Imperialist competitive algorithm has been utilized in [18] to solve a profit based unit commitment (UC) problem where the objective is to maximize profits under emission constraints over a 24-h interval. In [19], the authors propose a method to include emission constraints in the EED model and utilizes the shadow pricing concept for optimal dispatch.

A number of formulations have been attempted to incorporate wind power in EED model [20–23]. In a widely used concept presented in [20], overestimation and underestimation costs are included in dispatch model for wind-thermal systems. In another approach explained in [21], the probabilistic characteristics of wind power are included in the model in the form of constraints. Alternatively, a wait-and-see approach incorporates the probabilistic characteristic of the problem in the probability density function (pdf) of the solution [22]. In the above three approaches thermal pollutant emissions are not considered. In another work [23], the effect of wind power on emission control is investigated, where incomplete gamma function for wind power model is used. However, the capability of wind integration on reducing emission has not been quantified in the above work. Among evolutionary approaches, the wind integrated EED is solved using evolutionary algorithm based on decomposition (MOEA/D) in [24]. Similarly, a gravitational acceleration enhanced particle swarm optimization (GA-PSO) is proposed in [25] for solution of EED problem with wind power. In the previous two works, in some scenarios used by the authors, emission have increased after wind integration although cost reduction is achieved. Further, a multi-period multi-objective optimal dispatch is utilized in [26], but no attempt is made to compare the cost and emission before and after wind integration. The concept of carbon savings as the difference between business-as-usual (BAU) emissions and emissions with renewable integration is used in [27], however, the work solely focuses on wind power modelling and optimization techniques. Two different PDFs represented in the form of available wind generation and dispatched wind generation are considered in [28] but no attempt is made to quantify the emission reduction capability of wind power. The authors in [29] perform scheduling for a system containing four hydro plants, ten wind power plants and three thermal power plants where the focus is on developing a new stochastic optimization algorithm for hydro-wind-thermal scheduling but emission reduction capability of wind integration in conventional power systems is not discussed. Thus, it is observed from the above mentioned literature that in most of the similar works by integrating wind farms into standard test systems, researchers have not given adequate focus to analyze the benefits of wind farm integration, particularly in terms of savings in cost and emission. In some of the cases the inclusion of wind units have only managed to reduce the cost but the solutions have resulted in increased emission. Also, no attempt has been made to quantify the cost savings and emission reduction after wind integration. Further, no previous research has incorporated the turbine performance index (TPI) [30] into the problem of EED, which may lead to a more realistic estimation of cost savings and emission reduction. Finally, this work is novel in comparing the estimated emission reduction with the actual emission reduction after wind integration.

In this context, the objective of the present work is to investigate the impact of wind turbine ratings and EED on cost savings (CS) and emission reduction (ER) in wind-integrated power systems. For this, a cluster of two wind farms are integrated in each of the three test power systems. EED is performed with power output of the wind farms at different rated power and TPI of the turbine. The contributions of the current work are stated as follows.

1. Unlike previous works, a comparison is made between cost and emissions before and after wind power is incorporated in the EED model, thereby quantifying the CS and ER capability of the wind power.
2. Emission factor of the test power systems is calculated which is then used to compare the estimated ER from wind power with actual ER which occurs when wind power is incorporated in the EED model.
3. For sensitivity analysis, the rated power and TPI of the wind turbines used in the wind farm are varied and their impact on CS and ER is analysed.

The rest of the paper is organized as follows. Section 2 presents the background of the methodology used for the work, where it essentially focuses on reviewing some fundamental concepts related to wind power generation and its integration. The exact problem set up and the characteristics of the problem are defined in Section 3. The solution methodology adopted in this work has been elaborated in Section 4. Section 5 elucidates several results obtained and draws inferences out of them. Finally, Section 6 concludes the paper and identifies future scopes in this work.

2. Background

In the current work, wind speed is modelled using Weibull distribution and linear power curve model of the turbine is used to calculate power output and energy capture. The impact of change in turbine characteristics i.e. rated power and TPI on cost and emission is investigated. The concept of emission factor is also used to evaluate the emission reduction as compared to estimated. The approach of this work is restricted to EED only and tools provided in *MATLAB* are used to obtain the same. The details are described below.

2.1. Wind speed simulation

The Weibull distribution described in (1) and (2) has been found to give a good representation of the variation in hourly mean wind speed over a year [31].

$$f(v) = k\frac{v^{k-1}}{c^k}\exp\left(-\left(\frac{v}{c}\right)^k\right) \tag{1}$$

$$F(v) = \exp\left(-\left(\frac{v}{c}\right)^k\right) \tag{2}$$

where $f(v)$ and $F(v)$ are respectively PDF and CDF of Weibull distribution, v is the wind speed, k is the shape parameter describing the shape of the distribution and c is the scale parameter, which is more important in energy calculations.

A number of methods have been suggested for estimating parameters of Weibull distribution. Some of the commonly used methods are graphical method, maximum likelihood method (MLE), modified MLE, moment method, equivalent energy method and wind energy pattern factor method [32]. Intelligent parameter estimation algorithms have also been utilized for Weibull parameter estimation [33]. Once the Weibull parameters are determined using the above methods, wind speed can be simulated using inverse transform method [34] following Weibull distribution as described in (3).

$$X = F^{-1}(U), \quad U \sim (0, 1) \tag{3}$$

where X is the random variable to be simulated i.e. wind speed and F is the CDF of the random variable i.e. (2).

Other distributions have also been used for describing wind speed variations such as gamma distribution, log-normal distribution, inverse Gaussian distribution and squared Normal distribution; wind speed can also be characterized and simulated without assuming any probability distribution [35]. However, the variable of significance for EED is not wind speed but wind power. The wind turbine power output depends on wind speed at turbine hub height which is significantly higher than the measurement heights of meteorological towers. Wind speed varies with height and the rate of increase with height depends on the terrain and climatological factors. Therefore, appropriate techniques must be used to extrapolate the wind speed to hub height. In one approach, the wind speed is extrapolated to hub height using power law whereas in another approach, parameters of Weibull distribution are extrapolated directly [36].

2.2. Power output and energy capture

Three main factors which influence the power output of a wind turbine are: wind speed distribution of the selected site, the tower height and power conversion characteristics of chosen wind turbine. The above values are not constant and change with wind speed and wind turbine settings. Fundamental wind power equation based modelling methods are difficult to use and do not correctly represent the behaviour of the wind turbines. Wind turbine power curves provided by the manufacturers are considered to be quite accurate to find the power output at various wind speeds of which a mathematical model can be developed using a number of curve fitting techniques [37]. The present study uses a liner power curve model, described in (4). Once the power output is available, the energy capture can be calculated from simulated wind data using (5) [38].

$$P_0 = \begin{cases} 0, & \text{for } v < v_c \\ P_r \frac{v - v_c}{v_r - v_c}, & \text{for } v_c < v < v_r \\ P_r, & \text{for } v_r < v < v_f \\ 0, & \text{for } v > v_f \end{cases} \tag{4}$$

where P_0 is the power output of the wind turbine, v_c, v_r and v_f are cut-in, rated and furling speeds respectively.

$$E_{TS} = \sum_{i=1}^{N} P_{0,i}\Delta t_i \tag{5}$$

where E_{TS} is the total energy output over a time period N from the simulated data and $P_{0,i}$ is the output of the wind turbine at time i.

2.3. Turbine performance index

One of the objectives of the current work is to perform a sensitivity analysis on the impact of change in wind turbine parameters on CS and ER. Apart from P_r, the turbines are classified in terms of turbine performance index (TPI) and their impacts are analysed. A brief description of the above index is presented below. Wind power production from a turbine is dependent on the following important turbine parameters viz. the cut-in speed (v_c), rated speed (v_r), furling or cut-out speed (v_f) and hub height (h). For a given location with known values of k and c parameters at hub height, the values of v_r, v_c and v_f can be so chosen to ensure optimal energy production. If v_r is very low, much energy can be ignored at higher wind speeds and vice versa. The TPI is obtained from normalized power curve and capacity factor curves for different values of normalized rated speed (v_r/c). A particular site has a unique TPI curve which can be used for comparison between different turbines. As the reference site used in this study has $k = 2.2$, the NP, CF and TPI curve for the same is plotted in Fig. 1.

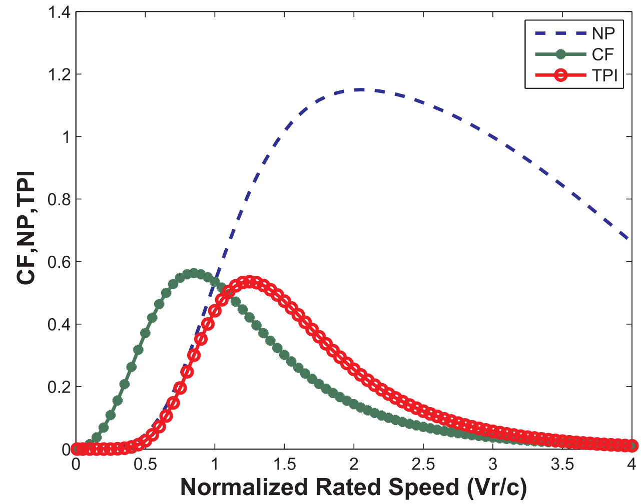

Fig. 1. Normalized power, capacity factor and TPI curves for $k = 2.2$.

2.4. Emission factor

Renewable energy developers aspiring to obtain assistance under CDM must calculate estimated emission reductions for the project under consideration. A CDM project is considered additional if anthropogenic emissions of greenhouse gases (GHG) are reduced as compared to the baseline scenario, which is when the project is not implemented i.e. it is the business-as-usual (BAU) scenario. For demonstrating the baseline and additionality the CDM projects must resort to available methodologies. The CDM methodologies appliable for grid connected renewable energy generation are 'Large-scale Consolidated Methodology (ACM0002)' for projects having installed capacity (IC) more than 15 MW and 'Small scale CDM Methodology (AMS-I.D.)' for IC < 15 MW respectively [3]. It can be observed from the project design documents (PDD) implementing above methodologies that the estimated emission reduction is simply the product of expected energy generation over a period and emission factor of the grid to which the project is planned to be integrated [4]. The emission factor for an electricity grid can be calculated using [39]. Based on procedure used by the CDM registered projects and grid emission factor calculation, the emission factor for the test power systems is defined in (6) and the estimated emission from energy capture values over a selected period TS is calculated using (7).

$$EF_{tps} = \frac{\sum_m Emissions_{m,y}}{\sum_m EG_{m,y}} \tag{6}$$

$$ER_{est} = E_{TS} * EF_{tps} \tag{7}$$

where EF_{tps} is the emission factor for the test power systems, the numerator is the total emissions from the m thermal generating units over a period y and the denominator is the total energy generated by m thermal generating units over the same period y, ER_{est} is the estimated emission reduction and E_{TS} is the estimated energy capture over a period TS.

2.5. Economic emission dispatch

The problem of EED in power system aims at obtaining a schedule of generating units to achieve optimal costs of generation and emission. The EED problem described in (8) to (12) is a non-linear, non-convex multi-objective optimization problem with two different objectives.

$$\begin{aligned} &Minimize \quad [F(P_i), E(P_i)] \\ &Subject\ to \\ &g(P_i) = 0 \\ &h(P_i) \leqslant 0 \end{aligned} \tag{8}$$

where

$$F = \sum_{i=1}^{N} a_i + b_i P_i + c_i P_i^2 + |d_i sin(P_i^{min} - P_i)^2| \tag{9}$$

$$E = \sum_{i=1}^{N} \alpha_i + \beta_i P_i + \gamma_i P_i^2 + \eta_i exp(\delta_i P_i) \tag{10}$$

$$P_i^{min} \leqslant P_i \leqslant P_i^{max} \tag{11}$$

$$\sum_{i=1}^{N} P_i = P_D + P_L \tag{12}$$

where F is the fuel cost of generation in (\$/h); E is the emission in (ton/h or lb/h); N is the number of thermal generators; P_i is the real power output of the ith generator; a_i, b_i, c_i, d_i and e_i are the coefficients of the ith generator fuel cost characteristics; α_i, β_i, γ_i, η_i and δ_i are the coefficients of the ith generator emission characteristics; P_D is the total electric power demand and P_L is the real power loss in transmission lines. Emission objective (10) can further be expanded into CO_2, SO_2 and NO_x emissions as in (13)–(15) which can also be added as separate objectives based on environmental regulation of the area where the power plant is located.

$$E_{CO_2} = \sum_{i=1}^{N} \alpha_{1i} + \beta_{1i}P_i + \gamma_{1i}P_i^2 + \eta_{1i}exp(\delta_{1i}P_i)\ ton/h \tag{13}$$

$$E_{SO_2} = \sum_{i=1}^{N} \alpha_{2i} + \beta_{2i}P_i + \gamma_{2i}P_i^2 + \eta_{2i}exp(\delta_{2i}P_i)\ toh/h \tag{14}$$

$$E_{NO_x} = \sum_{i=1}^{N} \alpha_{3i} + \beta_{3i}P_i + \gamma_{3i}P_i^2 + \eta_{3i}exp(\delta_{3i}P_i)\ ton/h \tag{15}$$

2.6. Wind integrated EED

The variability of wind power is the primary limitation for scheduling decisions in wind-integrated power systems. The current study uses the method described in [20] for incorporating wind power scheduling in the EED model. The above work has introduced two cost factors to account for the risk of overestimating and underestimating wind power. A brief description of the above concept is presented as follows. If the power generation from wind is overestimated compared to the actual availability, then the shortfall of power generation must be compensated from other areas or system reserve, which incurs a cost. Similarly, in the event of underestimated wind power generation, some amount of the same would be wasted, for which the system operator may pay a cost in the form of a penalty levied on him by the wind farm owner for violating the wind power integration policy framework. In the worst scenario, surplus wind power may be lost in dummy resistors. The above wind power model is restated in (16) for ready reference.

Minimize

$$\sum_{i=1}^{N} C_i(P_i) + \sum_{i=1}^{M} C_{wi}(w_i) + \textstyle\sum_{i=1}^{M} C_{p,w,i}(W_{i,av}-w_i) + \displaystyle\sum_{i=1}^{M} C_{r,w,i}(w_i-W_{i,av}) \tag{16}$$

Subject to

$$P_i^{min} \leqslant P_i \leqslant P_i^{max}$$
$$0 \leqslant w_i \leqslant w_{r,i}$$
$$\sum_{i=1}^{N} P_i + \sum_{i=1}^{N} w_i = L \tag{17}$$

where

N is the number of thermal generators,
M is the number of wind powered generators,
w_i is the scheduled power from ith wind powered generator.
$W_{i,av}$ is the available wind power from ith wind powered generator.
w_i rated wind power from the ith wind powered generator.
C_i is the cost function of the ith conventional generator.
$C_{p,w,i}$ is the penalty cost function for not using all available wind power from ith wind powered generator.
$C_{r,w,i}$ reserve cost associated with overestimation of wind power.
L represent the total system load and losses.

In Eq. (16), the first term is the fuel cost, the second term the direct cost of wind generation, the third term accounts for not using the available wind power and the fourth term is for the penalty for underestimation of wind power.

In general, distributed generation (DG) resources such as wind generation are inherently intermittent in nature. This introduces considerable uncertainty into the generation scheduling as the actual amount of wind power availability is not certain. As discussed in this section, DG intermittency is accounted for by using overestimation and underestimation cost in the WEED model. It is worthwhile to mention here that increase in DG penetration effectively reduces the impact of intermittent nature of renewable generation [40].

3. Problem formulation

The exact problem setup to obtain CS and ER is to evaluate the terms defined in (18a) to (18d) for the selected test systems.

1. *Cost Savings (CS)*: it is defined as the difference between the costs before (C_{bw}) and after (C_{aw}) the inclusion of wind power in the EED model as a percentage of cost before wind inclusion (18a).
2. *Emission Reduction (ER)*: it is defined as the difference between emission before (E_{bw}) and after (E_{aw}) the wind power is included in EED as a percentage of emission before wind inclusion (18b).
3. *Emission Reduction compared to estimated* (ER_{ef}): it is defined as actual emission reduction with wind integration as a percentage of the estimated emission reduction (ER_{est}) (18c).
4. *Wind Energy Share (WES)*: it is defined as the share of wind energy (E_W) in the total energy (E_{WT}) (wind and thermal) consumed by load in the selected time period (18d).

$$CS = \frac{C_{bw}-C_{aw}}{C_{bw}} \times 100 \tag{18a}$$

$$ER = \frac{E_{bw}-E_{aw}}{E_{bw}} \times 100 \tag{18b}$$

$$ER_{ef} = \frac{E_{bw}-E_{aw}}{ER_{est}} \times 100 \tag{18c}$$

$$WES = \frac{E_W}{E_{WT}} \times 100 \tag{18d}$$

4. Solution methodology

The first step towards evaluating terms defined in (18a) to (18d) is the estimation of wind power for each scheduling interval. This requires simulation of the marginal distribution (3) and calculation of power outputs (4). In this work, the parameters of the Weibull distribution are assumed based on [25]. When the parameters of the underlying distribution are not available those can be obtained by the methods discussed in [32]. Once the power outputs are obtained, evaluation of ER_{est} is done using (7). The cost and emission before wind integration C_{bw}, E_{bw} and after wind integration C_{aw}, E_{aw} are obtained from the solution of the EED problem (8). EED with wind power involves the overestimation and underestimation costs and hence requires the solution of (16).

The MC and ME solution of (8) and (16) is obtained using `fmincon` function of MATLAB Optimization Toolbox. Specifically, the solution of (16) is obtained by including C_p and C_r in the objective function definition. It is to be noted here that `fmincon` includes the solution of Karush-Kuhn-Tucker (KKT) equations. However, the focus of this work is not to obtain global optimum and the solution obtained using `fmincon` is close, when compared to those reported in past literature for the considered test system with regards to practical importance of

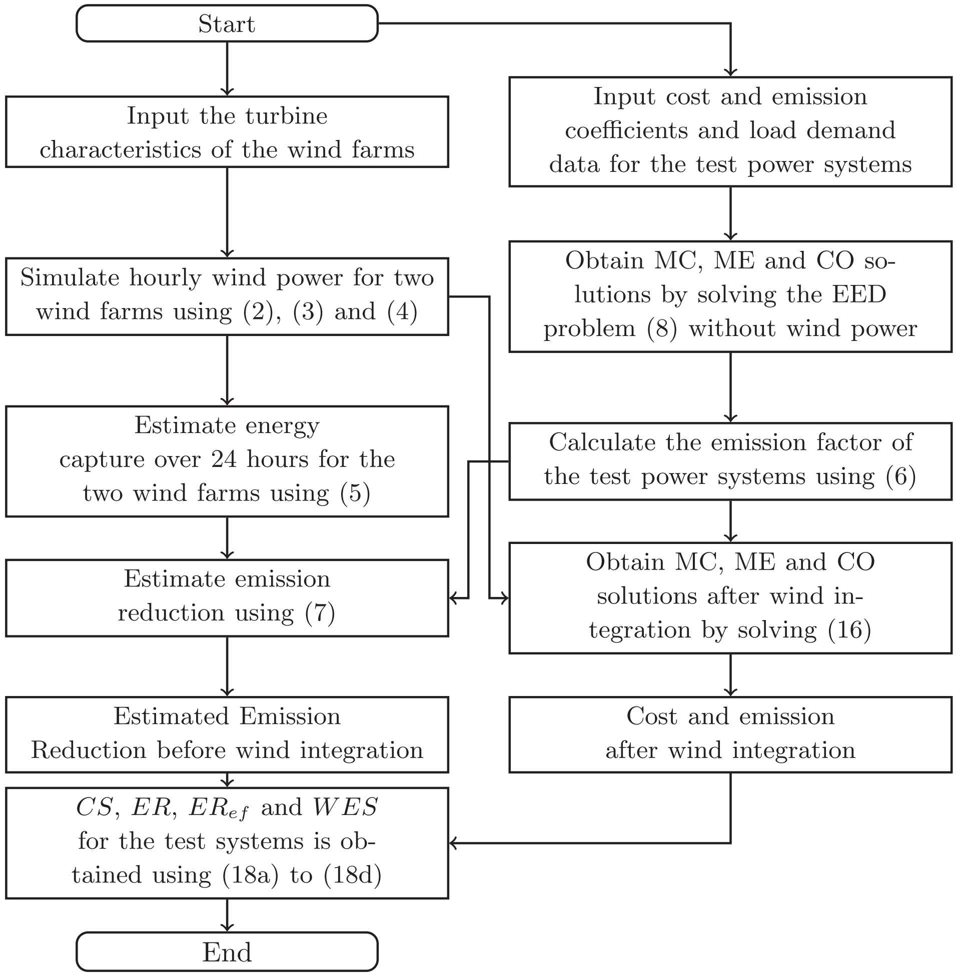

Fig. 2. Solution methodology.

the problem. To obtain the multiobjective solution, `gamultiobj` function of MATLAB Global Optimization Toolbox is used to obtain the pareto front. For the large scale system, in order to reduce computational burden, the pareto front is obtained using `fgoalattain` fuction of MATLAB Optimization Toolbox. The final solution to the multiobjective problem is obtained by using fuzzy membership function of each solution of the pareto front as described in [10]. As the above solution is a compromise between both cost and emission objectives, it is referred as compromise solution (CO). The resultant cost and emission from MC, ME and CO solutions before and after wind integration are used to evaluate (18a) to (18c). Further, as described in section 'Emission factor', the ER_{est} in (18c) is obtained from the energy capture estimates and emission factor of the test power systems.

The solution approach is summarized in the following steps. The same is depicted pictorially in Fig. 2.

1. For each of the test systems, the MC and ME solutions are obtained using nonlinear programming with interior-point algorithm. For the multiobjective case (8), a set of pareto optimal solutions is obtained and the best compromise solution (CO) is obtained using fuzzy based selection technique as described in [10].
2. The emission factor of the test systems is obtained from the MC, ME and CO solutions using (6).
3. Two wind farms based on [25] were chosen and wind power outputs were obtained using (2), (3) and (4). For each of the wind farms different sets of wind power outputs were simulated by varying the P_r and TPI of the turbines.
4. The energy capture and emission reduction estimates of the wind farms for 24 h period is calculated using (5) and (7).
5. The power outputs of the two wind farms are included in the dispatch model (16) and ME, MC and CO solutions for the selected period are obtained after wind integration.
6. Finally, the CS, ER, ER_{ef} and WES due to wind-integration in the EED model are obtained using (18a) to (18d) from the solutions obtained in steps 1 and 5.

Day ahead scheduling as in [16,17,26,28] is considered in this paper to demonstrate a methodology for evaluating CS and ER capability of a wind-integrated power system. As this paper does not aspire to examine forecasting techniques, these day ahead scenarios are obtained by simulation of Weibull distribution. It is noteworthy to mention here that stochastic frameworks such as point estimate method [41] can be used to represent large number of scenarios. However, it is out of the scope for this work as it is concerned only with day-ahead CS and ER.

5. Results and discussion

At the outset, the most relevant results available in recent literature are reproduced in Table 1 for ready reference. The units of cost and emission are not included deliberately as the objective is comparing the values before and after wind integration. The results provided for [24–26] are for IEEE 30 bus 6 generator system. The solution in [24] includes losses and security constraints whereas the solution in [25] is for the lossless scenario. It can be observed that after wind integration in [24], the hourly emission is increased and hourly cost is decreased for all types of solution. In [25], the hourly emission is increased and

Table 1
Relevant results from recent literature.

Sl.	Ref.	Sol. type	No Wind		With Wind	
			Cost	Emission	Cost	Emission
1	[24]	MC	619.53	0.2017	583.92	0.2195
		ME	644.98	0.1942	627.11	0.1943
		CO	625.69	0.1964	595.36	0.1993
2	[25]	MC	600.29	0.2221	471.89	0.2458
		ME	638.26	0.1942	657.57	0.1936
		CO	615.38	0.1978	572.19	0.2049
3	[26]	MC	NA[#]	NA	80264	229.33
		ME	NA	NA	93941	149.11
		CO	NA	NA	86233	179.49
4	[9]	MC	64083	1345.6	NA	NA
		ME	65991	1240.7	NA	NA
		CO	64843	1286	NA	NA
5	[9]	MC	111500	4581	NA	NA
		ME	116400	3293.4	NA	NA
		CO	113480	4124.9	NA	NA
6	[9]	MC	121840	374790	131701	335548
		ME	129960	176680	158269	156826
		CO	125790	211190	146035	172268

[#] Not Available in the literature.

hourly cost is decreased for MC, CO solution whereas the results are opposite in case of ME solution. In [26], no attempt is made to compare the increase or decrease in cost or emission after wind integration over scheduling interval of 24 h. The systems 4 and 5 provided in Table 1 are for a 6 and 10 generator system respectively where losses are calculated using B-coefficients. These two systems are chosen in the current work because of the specific generator characteristics. The last system shown in Table 1 is a large scale 40 generator system and it can be observed that in all of the MC, ME and CO solutions, there is increase in cost and reduction in emission after wind integration. Thus in all the system described so far the impact of wind integration is different and the current work is novel in the sense that a systematic investigation is done on the CS and ER due to wind integration. Further, the turbine characteristics (P_r and TPI) of each wind farm are changed to generate various scenarios and the impact of each of these scenarios on CS and ER is investigated. The scenarios are depicted in a pictorial form in Fig. 3 and described in Table 2.

5.1. Test power systems

The test systems are selected so as to include a wide range of generator cost and emission characteristics. A brief description of the test systems is described below.

Test system A: The first test power system is a 6 generator system provided in [9]. In this system the cost and emission characteristics of generators is quadratic. The load is assumed to be constant at 1200 MW for 24 h.

Test system B: The second test power system is the IEEE 30 bus 6 generator system described in [7]. In this system the cost characteristics of generators is quadratic, but the emission characteristics is a combination of quadratic and exponential functions. The load is assumed to be constant at 2.834 pu on a 100 MW base.

Test system C: The third test power system is a 10 thermal generator system as described in [9]. In this system, the cost characteristics contain quadratic and a sinusoidal term representing valve-point loading effects. The emission characteristics is sum of a quadratic and an exponential term. The load is assumed to be constant at 2000 MW for 24 h.

Test system D: To show the scalability of the proposed approach, a 40 thermal generator system [9,25] is included as the fourth test power system. In this system, the cost characteristics contain quadratic and a sinusoidal term representing valve-point loading effects. The emission characteristics is sum of a quadratic and an exponential term. The load is assumed to be constant at 10500 MW for 24 h.

Table 2
Summary of test scenarios.

Test system	A		B		C		D	
Variation in	Power	TPI	Power	TPI	Power	TPI	Power	TPI
Scenario	A1	A2	B1	B2	C1	C2	D1	D2

5.2. Base case without wind integration into the test systems

Initially the test power systems are considered without wind power integration. EED is performed to obtain MC, ME and CO solutions. From the emission values the emission factor is calculated using the procedure described in Section 4. Losses are not relevant to the current study and hence these are conveniently neglected. It must be reiterated here that MC, ME and CO solutions are already available in literature for these test systems as these have been used by several authors to verify their proposed optimization technique. Nevertheless, the solutions are obtained again using the optimization method used in this work to enable comparisons with wind-integrated case. The base case results are provided in Table 3 and it is found that these results are comparable to those reported in literature [9,25] and their accuracy may be sufficient as far as the objectives of the current study are concerned. For the sake of comparison, the hourly generation schedules, cost and emission of

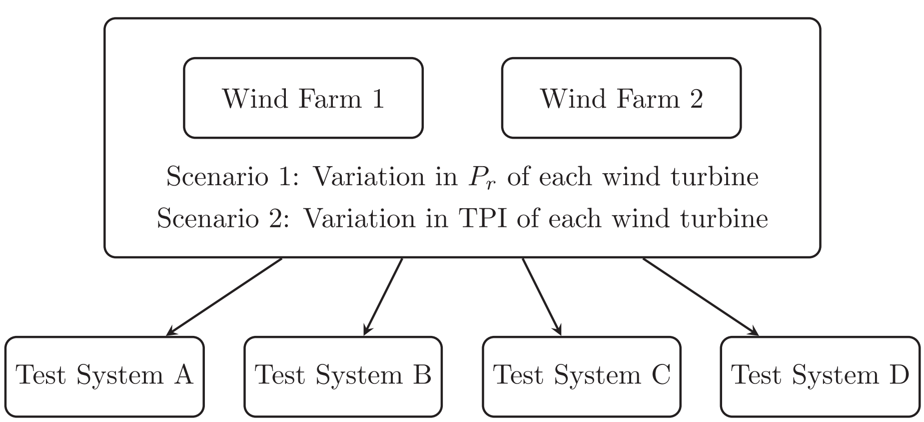

Fig. 3. Description of various scenarios.

Table 3
Emission factor of the test systems.

Test system	Solution type	Cost ($/h)	Emission (units/h)[a]	E.F. (units/MWh)[b]	Total Load (MW)
A	MC[c]	60809.22	1294.73	1.07894004	1200
	ME[d]	63485.10	1135.68	0.94640482	1200
	CO[e]	62231.68	1176.87	0.98073076	1200
B	MC	600.1114	0.2221	0.00078386	283.4
	ME	638.3807	0.1242	0.00068526	283.4
	CO	607.3861	0.2038	0.00071915	283.4
C	MC	106170.4	4278.76	2.13937980	2000
	ME	111867.5	3650.74	1.82537030	2000
	CO	110497.4	3880.03	1.94001658	2000
D	MC	124474	346740	33.023	10500
	ME	129954	176682	16.827	10500
	CO	126551	188453	17.948	10500

[a] lb/h for test systems A and C, ton/h for test system B and D.
[b] lb/MWh for test systems A and C, ton/MWh for test system B and D.
[c] Minimum cost.
[d] Minimum emission.
[e] Compromise solution.

the thermal generating units are provided in Tables A1 to A4 of Appendix A for test systems A, B, C and D respectively. The results from the existing state-of-the-art are also provided. It can be observed that the optimal schedules, MC, ME and CO solutions obtained using the selected methods are comparable to the existing state-of-the-art and thus proving their suitability for the current study.

5.3. Turbine characteristics

Two wind farms are chosen to be integrated into each of the test power systems. Each wind farm contains a cluster of 50 turbines. As described earlier, various scenarios are generated by changing the P_r and TPI of the turbines of the wind farm. For scenarios A1, B1 and C1, P_r of the turbines used in the wind farm is varied from 500 kW to 2500 kW thus varying the installed capacity of each wind farm from 25 MW to 125 MW. Hence by varying the wind turbine P_r, the IC of two wind farms as a percentage of test power system load vary from 4.17% to 20.83% for system A, 17.64% to 88.21% for system B and 2.5% to 12.5% for system C. In the large scale test system D, two clusters of wind farms are considered where each cluster has ten wind farms. These clusters are assumed to be dispatched as a single generator. Thus IC of the each cluster of wind farms varies from 250 MW to 1250 MW making the total wind IC vary from 4.76% to 23.81% of the system load. In the second set of scenarios A2, B2 and C2, the wind turbine rated power is fixed at 2500 kW, i.e. for these scenarios the installed capacity of each wind farm is 125 MW. For scenarios D1 and D2, the IC of each cluster of wind farms is fixed at 1250 MW. The TPI of each of the turbines used in the wind farms is varied by varying the turbine v_r from 8 m/s to 18 m/s in steps of 0.5 m/s. This results in a minimum TPI of 0.1492 for v_r = 8 m/s and maximum TPI of 0.4107 for v_r = 18 m/s. The TPI for other turbine rated speeds can be inferred from Fig. 1. Wind power outputs were obtained for each wind farm for each of the wind turbine characteristics. This results in 21 sets of hourly power outputs when rated power is varied and another 21 sets of power outputs when TPI is varied. These sets of power outputs of the wind farms are be used in the EED of wind-integrated test power systems. Also, these power outputs are used to compute energy capture over a 24-h period which when combined with the emission factor from Table 3 provides the ER_{est} from the two wind farms that in turn is used to compute ER_{ef}.

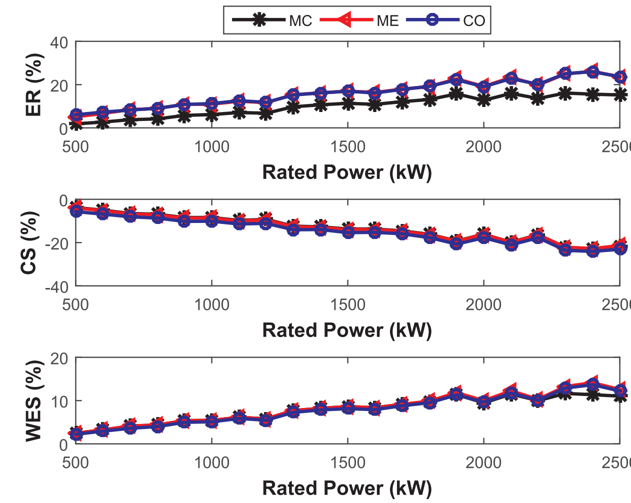

Fig. 4. CS, ER and WES for Scenario A1.

Table 4
Min and Max values of ER, CS and WES.

Sce.	Sol. type	ER (%)		CS (%)		WES (%)	
		Min	Max	Min	Max	Min	Max
A1	MC	1.84	16.11	−23.04	−3.78	2.45	11.65
	ME	5.10	26.12	−22.77	−3.96	2.45	14.13
	CO	6.07	25.97	−24.06	−5.68	2.22	13.67
A2	MC	11.58	17.78	−23.41	−14.29	8.64	12.71
	ME	17.25	26.85	−23.27	−14.46	8.87	14.33
	CO	16.97	27.11	−24.61	−15.78	8.45	14.00
B1	MC	−9.00	−0.27	4.58	17.16	11.25	58.50
	ME	0.00	0.00	−25.94	−4.96	0.01	0.02
	CO	−5.67	0.27	−7.12	0.71	8.94	29.01
B2	MC	−9.66	−4.21	12.17	19.29	36.25	61.56
	ME	0.00	0.00	−27.30	−16.06	0.01	0.02
	CO	−4.65	−0.40	−6.72	−0.58	22.12	32.92
C1	MC	2.63	13.30	−12.25	−2.33	1.62	8.38
	ME	2.88	13.94	−12.17	−2.33	1.62	8.38
	CO	2.89	13.16	−13.57	−3.99	1.29	7.79
C2	MC	9.20	14.79	−13.63	−8.43	5.86	9.31
	ME	9.99	15.43	−13.53	−8.39	5.86	9.31
	CO	8.80	14.87	−14.50	−9.75	5.41	8.63
D1	MC	24.18	62.97	3.00	18.29	4.76	23.71
	ME	24.92	70.77	4.98	17.47	4.76	23.81
	CO	15.96	56.35	2.36	10.63	3.06	15.01
D2	MC	41.78	76.84	15.41	19.81	20.97	23.81
	ME	70.77	70.77	16.93	19.25	23.81	23.81
	CO	47.05	66.88	3.34	15.42	11.48	20.55

5.4. Cost and emission after wind integration

The plots of CS, ER and WES with variation in P_r and TPI of the turbines of the wind farm are shown in Fig. 4 to Fig. 11. The maximum and minimum values of the same are provided in Table 4. It must be noted here that these maximum and minimum values might have occured for any P_r or TPI value and not necessarily the first and last values.

5.4.1. Test system A

It can be observed from Fig. 4 that, for MC solution, with increase in P_r of the turbines of the wind farm, the ER increases from 1.84% to

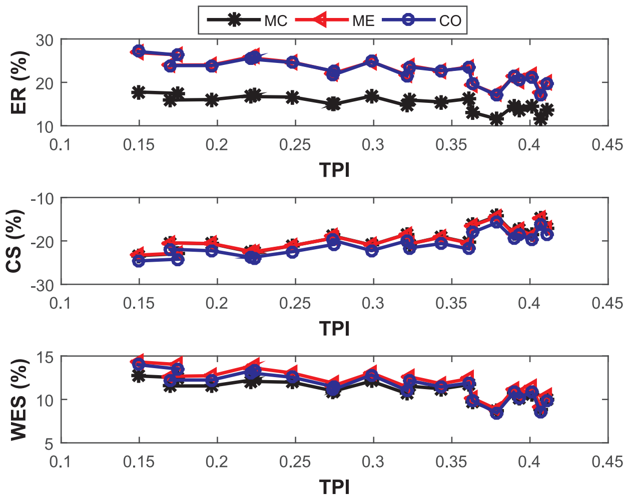

Fig. 5. CS, ER and WES for Scenario A2.

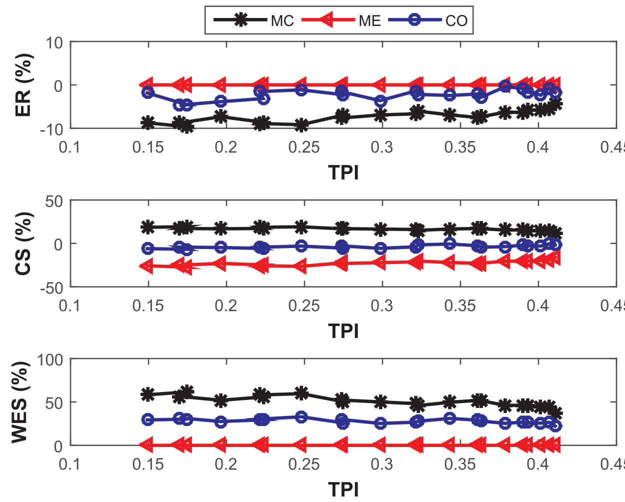

Fig. 7. CS, ER and WES for Scenario B2.

16.11%. This is expected since the increase in P_r of the wind turbine increases the wind farm capacity and hence the energy output of the farm. This is also evident from the WES values which increases from 2.45% to 11.65% as the P_r is increased. However, an increase in WES is general but not necessarily followed e.g. WES with $P_r = 2300$ kW is 11.65% whereas that with $P_r = 2500$ kW is 11.04%. The CS, contrary to ER, has decreased from -3.78% to -23.04% with increase in P_r. Thus the integration of wind power is costlier although there is a significant increase in ER. For ME and CO solutions, the values of ER, CS and WES follows similar pattern as in MC solution. For scenario A2, Fig. 5 plots ER, CS and WES values with increase in TPI of the turines. It can be seen from the above plot that ER increases from 11.58% to 17.78% when TPI of the turbine is increased, but this increase is not linear. There is a general increase in CS with TPI, but it is still negative. WES does not seem to have any definite relationship with TPI, but a gradual decrease in WES with increase in TPI is observed.

5.4.2. Test system B

Figs. 6 and 7 show the CS, ER and WES for test system B for variation in P_r and TPI respectively. In this test system, the results appear to be opposite to that of test system A. It can be observed from Fig. 6 that for MC solution, the ER is negative and decreases from -0.27% to -9% with increase in P_r. Thus an increase in the power rating of the turbine in test system B results in increase in emissions. The CS for MC solution increases from 4.58% to 17.16% with increase in P_r thus making wind integration in test system B quite cost effective. As with test system A, WES increases with increase in P_r. However, it can be observed that the ME solution has resulted in zero ER. This reason is evident in the WES values which is nearly zero for all P_r values. Thus, a counter-intuitive result is observed in test system B where wind energy is not preferred in ME solution the reason for which is enumerated shortly. The CO solution has resulted in nearly zero ER and CS except for a few values, CS being negative for a majority of wind turbine power rating. The WES, however, increases from 8.94% to 29.01% in general with increase in P_r, thus ensuring that wind energy has been included in the generation schedules in spite of nearly zero CS and ER or in other words, CS and ER compensate each other in CO solution. No perceptible variation in ER,CS and WES is observable with change in TPI as it is evident from Fig. 7. Also, with change in TPI, the CS is positive for only MC solution, WES is zero for ME solution and WES is highest for MC solution thus showing that wind-integration primarily results in cost reduction in test system B.

5.4.3. Test system C

The CS, ER and WES for test system C with variation in P_r and TPI are shown in Figs. 8 and 9 respectively fro MC,ME and CO solutions. The general trends for solutions in this test systems are similar to test system A. However, WES values are much less compared to that in test system A increasing from 1.62% to 8.38% for MC, ME solution and from 1.29% to 7.29% for CO solution with increase in P_r. This is because the

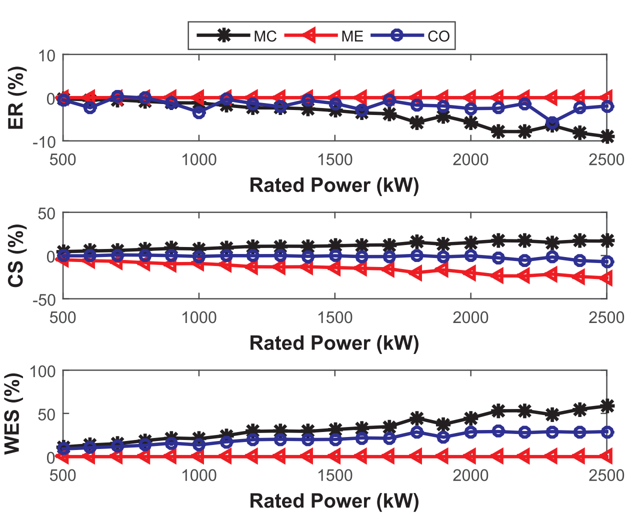

Fig. 6. CS, ER and WES for Scenario B1.

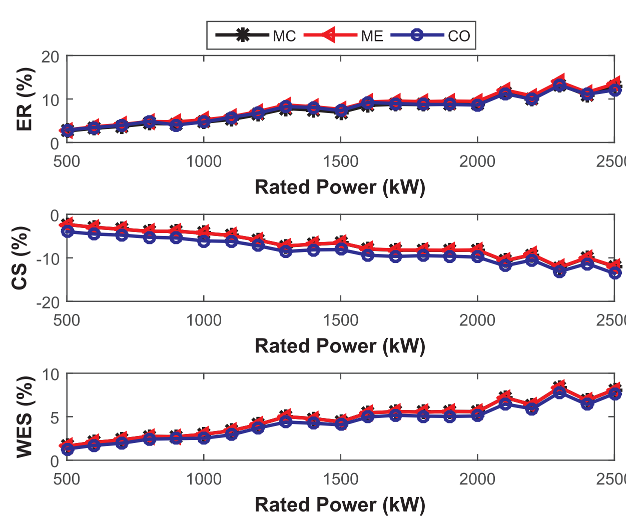

Fig. 8. CS, ER and WES for Scenario C1.

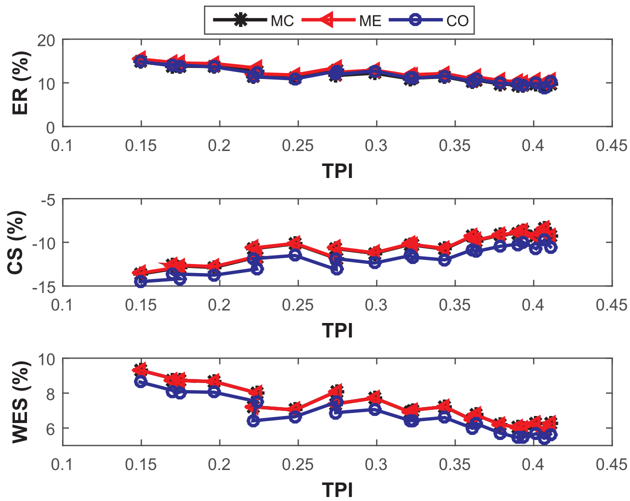

Fig. 9. CS, ER and WES for Scenario C2.

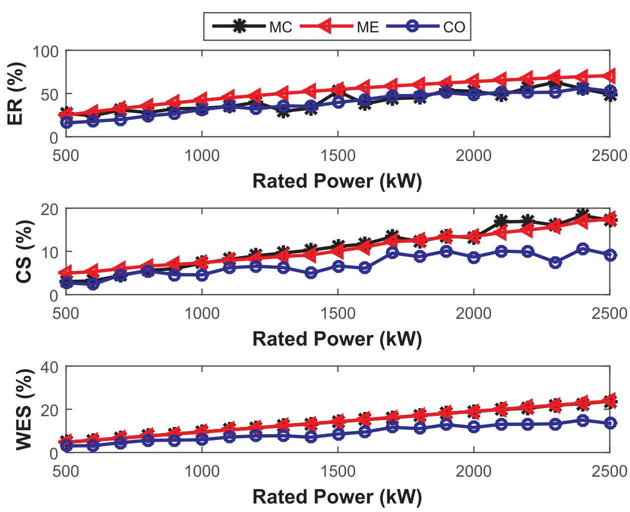

Fig. 10. CS, ER and WES for Scenario D1.

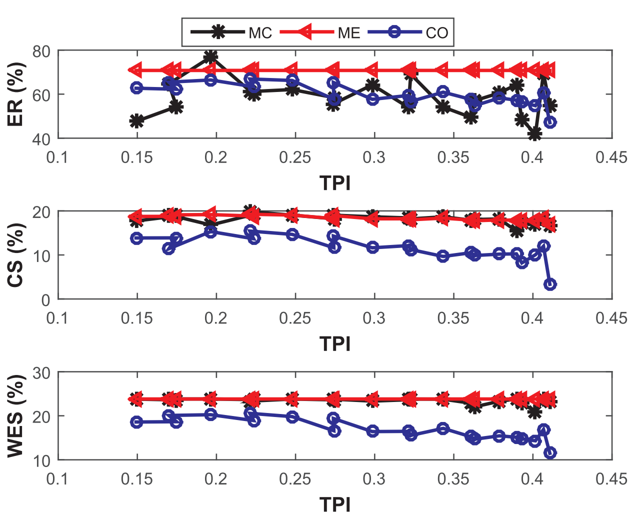

Fig. 11. CS, ER and WES for Scenario D2.

load here is higher than that of system A and thus making the minimum and maximum wind IC as 2.5% and 12.5% of the load for P_r of 500 kW and 2500 kW respectively. For MC solution, with increase in P_r, ER increases from 2.63% to 13.30% whereas CS is negative decreasing

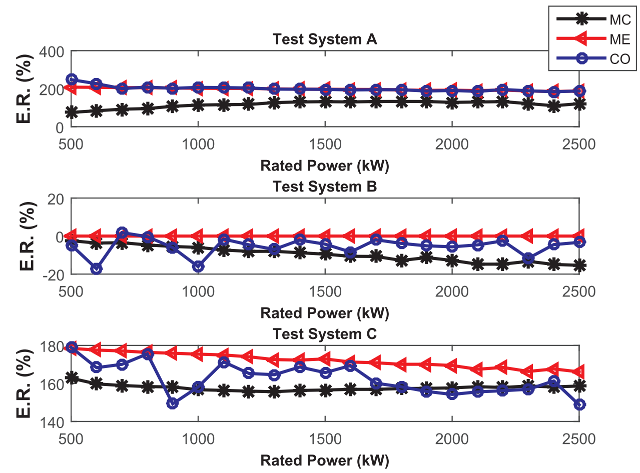

Fig. 12. Variation of emission reduction as (% of estimated) with rated power.

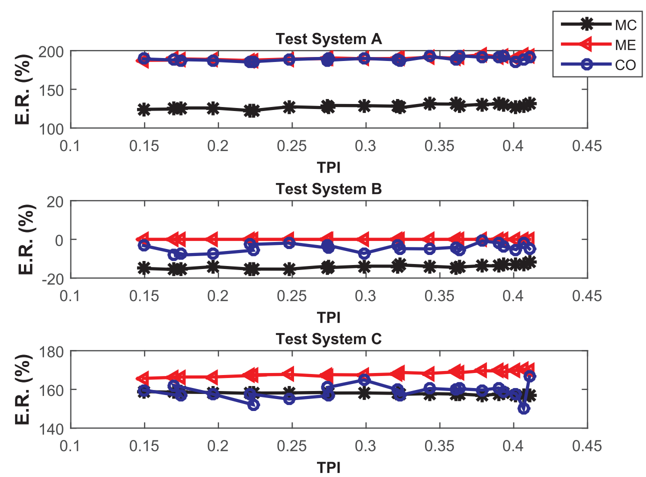

Fig. 13. Variation of emission reduction as (% of estimated) with TPI.

from −2.33% to −12.25%. Thus, in test system C, wind-integration is not cost effective, however, it can help reduce emissions. Another observation is that results for MC, ME and CO solutions are almost overlapping i.e. type of solution does not have much impact on ER, CS and WES in test system C. From Fig. 9, it can be observed that an increase in TPI has a general impact of reducing ER, increasing the CS and decrease in WES.

5.4.4. Test system D

The CS, ER and WES for the large scale test system D with variation in P_r and TPI are shown in Figs. 10 and 11 respectively. It can be observed from Fig. 10 that the WES values vary between 4.76% to 23.71% for MC solution, 4.76% to 23.81% for ME solution and 3.06% to 15.01% for CO solution. The WES values for MC and ME solutions almost overlap signifying no impact of MC or ME solution on generation schedule. This is due to a much lower value of direct cost of wind farms as compared to the fuel cost of thermal generators. The CS and ER values closely follow the WES values. The CS increases from 3% to 18.29% for MC solution, 5% to 17.47% for ME solution and 2.36% to 10.63% for CO solution. The ER increases from 24% to 63% for MC solution, 25% to 71% for ME solution and 16% to 56% for ME solution. It can be observed from Fig. 11 that change in TPI does not affect the CS, ER and WES for ME solution. For MC solution, the CS, ER and WES values vary from 15.41% to 20%, 42% to 77% and 21% to 24% respectively. Finally, for the CO solution, the variation of CS, ER and WES are between 3.34% and 15.42%, 47% and 67%, 11.48% and 20.55% respectively. Thus it can be observed that in a large scale system, though wind integration is cost effective, it has resulted in much higher values of ER compared to other test systems.

5.4.5. ER_{ef}

The preceding discussion primarily focuses on CS and ER where both these values are measured as a fraction of cost and emission without wind integration. But the primary objective of wind integration is reducing emissions and the above values do not provide much insight on the relationship between the actual and estimated emissions. Hence, the actual ER due to wind integration (E_{aw}–E_{bw}) as a percentage of the estimated ER (ER_{est}) i.e. ER_{ef} (Refer (18c)) is provided in Figs. 12 and 13 for variation in P_r and TPI respectively. When the P_r is varied from 500 kW to 2500 kW, the minimum and maximum values of ER_{ef} are (75.22%, 247.61%), (−2.42%, 1.82%) and (148.75%, 179.02%) for system A, B and C respectively. With change in TPI of the turbines of the wind farm, the minimum and maximum values of ER_{ef} are (122.22%, 194.67%), (−9.66%, 0%) and (150.18%, 170.44%) for test systems A, B and C respectively. The ER_{ef} values for test system D are similar to A and C and hence not included here. Thus in test systems A, C and D the actual emission reduction is more than the estimated value whereas in test system B it is very less as compared to estimated. not included here. ER_{ef} values of more than 100% might have been due to two factors contributing to emission reduction, the emission free wind energy and the de-loading of thermal units.

The following points are worth noting from the above discussion.

1. The cost savings and emission reduction as a percentage of cost and emission without wind integration are dependent on the generator characteristics of the test systems.
2. The cost and emission after wind integration may increase or decrease. It has been found that the cost saving is followed by increase in emission and vice versa.
3. Although an increase in power rating of the turbines results in increase in wind energy share it does not necessarily mean an increase or decrease in emission reduction.
4. Variation in turbine performance index i.e. of rated speed and capacity factor do not have much impact on cost and emission reductions. It is the power rating of the turbine which is more dominant in affecting these quantities. Thus in scenarios with variations with TPI, a nearly horizontal curve is obtained.
5. Emission reduction as a percentage of estimated value of emission, is nearly zero or negative in some test systems. The reason may be due the nature of generator emission characteristics where inclusion of wind energy is resulting in more emissions from thermal generators.
6. Emission reduction as a percentage of its estimated value of emission is more than 100% in some scenarios. The following explanation can be given for the above. The emissions for all the generators are taken together while calculating emissions. Energy available in the wind for 24 h as calculated from the power curve is utilized for emission reduction estimates. In wind integrated dispatch, for all types of solutions, the algorithm tends to schedule the total available power in the wind. This results in less output from the thermal generators and hence reduced emissions. This added with the zero emission wind power results in more than 100% emission reduction as compared to the estimated.

5.5. Sensitivity analysis

In this work, the CS and ER capability of wind integrated power systems is estimated by varying the P_r from 500 kW to 2500 kW in steps of 500 kW. It is observed that the impact of increase in P_r is dependent on thermal generator characteristics and hence is dependent on the power system in which the wind farm is integrated. Increase in P_r has resulted in increase in operational cost for test system A and C but decrease in cost in test system B and D; increase in ER for test system A, C and D, but decrease in ER for test system B. Also, the increase in P_r have resulted in increase in WES of the wind farms in all scenarios. The v_r of the turbines are increased from 8 to 18 m/s resulting in change in TPI. With increase in TPI, there is a general increase in CS and small reduction in ER for test system A and C, minor variations in CS and ER for test system D whereas no perceptible change in CS and ER is observed for test system B. Impact of change in direct, overestimation and underestimation cost with wind integration is covered in detail in [20] and hence not considered here.

5.6. Network constraints

Network constraints such as transmission losses, bus voltage profile, line flow limits has not been considered in this paper as the focus has been on capability of wind generation on reducing cost and emission. However, the approach remains the same although CS and ER capability of the wind power integration may be altered in the presence of network constraints. This can only be ascertained by detailed system studies which are out of scope for this paper and can be taken as a future work.

6. Conclusion

In this work, the cost savings and emission reduction due to wind integration is investigated in four test power systems. The concept of emission factor is invoked to compare the estimated emission reduction from wind energy with actual emission reduction in power systems. It is found that the response of each test power system to wind integration is different for same turbine characteristics of the wind farms. In the test system A, when both cost and emission characteristics are quadratic in nature, there is reduction in emission after wind integration while there is a corresponding increase in cost. In the test system B with quadratic cost characteristics but non-smooth emission characteristics, emission increases after wind integration whereas cost decreases. This is in spite of the fact that the farm capacity of wind energy as a percentage of load is highest in the test system B. In the test system C having non-smooth characteristics for cost and emission, there is decrease in emissions and increase in cost due to wind integration. In the large scale test system D, both cost savings and emission reduction are positive and higher compared to the other test systems. Finally, the emission reduction after wind integration is compared with the estimated values obtained from wind energy output and emission factor of the test power system. The emission reduction expressed as a fraction of estimated value of emission is sometimes more than 100% as in test systems A, C and D where as it is negative in test system B. Thus the emission reduction calculation based on average emission factors, as prevalent in many projects aspiring climate funds may be reformulated, so that estimated and actual values are nearer. It is further observed that no general conclusion can be made regarding the cost savings and emission reduction capacity of a wind farm when integrated to a power system and actual cost savings and emission reduction is dependent on the cost and emission characteristics of the generators as well as the solution type desired. Variation of rated power has more impact on cost savings and emission reduction as compared to variation in TPI. In summary, while estimating emission reduction from a wind energy project, a thorough investigation must be made for the power system in which such project is to be integrated. As a future work, the impact of other operational aspects of actual power system operation on the cost saving and emission reduction capability of wind power can be investigated.

Appendix A. Generation schedule and comparison with existing state-of-the-art

Table A1
Generation Schedule (MW) for Test system-A.

Unit	No Loss			With Loss			OGHS[#] [14]		
	MC	ME	CO	MC	ME	CO	MC	ME	CO
G1	65.97	125.00	97.02	87.75	125.00	104.24	83.75	125.00	105.73
G2	59.03	150.00	123.81	90.38	150.00	110.11	92.06	150.00	119.08
G3	210.00	187.88	203.61	210.00	198.01	202.38	210.00	200.28	205.30
G4	225.00	187.88	207.03	225.00	198.01	205.51	225.00	198.46	204.78
G5	315.00	274.62	291.61	315.00	289.64	315.00	315.00	286.59	305.80
G6	325.00	274.62	276.93	325.00	289.64	315.04	325.00	288.05	308.91
Cost	60809.22	63485.10	62231.68	64101.89	65981.98	64627.75	63953.08	65899.36	64722.74
Emission	1294.73	1135.69	1176.88	1345.79	1240.80	1299.23	1343.44	1236.77	1281.35

[#] Opposition-based greedy heuristic search.

Table A2
Generation Schedule (pu) and comparison for Test system-B.

Unit	No Loss			MOPSO[#] [8]			With Loss			MOPSO [8]		
	MC	ME	CO	MC	ME	CO	MC	ME	CO	MC	ME	CO
G1	0.1097	0.4059	0.2453	0.1183	0.4015	0.2516	0.1134	0.4095	0.2703	0.1207	0.4101	0.2367
G2	0.2998	0.4591	0.3286	0.3019	0.459	0.377	0.3027	0.4629	0.3613	0.3131	0.4594	0.3616
G3	0.5243	0.5354	0.5287	0.5224	0.5332	0.5283	0.5332	0.5434	0.4944	0.5907	0.5511	0.5887
G4	1.0162	0.3828	0.7292	1.0116	0.3891	0.7124	1.0222	0.3892	0.7218	0.9769	0.3919	0.7041
G5	0.5243	0.5373	0.6234	0.5254	0.5456	0.5566	0.5332	0.5434	0.5734	0.5155	0.5413	0.5635
G6	0.3597	0.5135	0.3787	0.3544	0.5057	0.4081	0.3633	0.5145	0.4432	0.3504	0.5111	0.4087
Cost	600.11	638.38	607.39	600.12	637.42	608.65	607.67	644.84	615.50	607.79	644.74	615
Emission	0.2221	0.1942	0.2038	0.2216	0.1942	0.2017	0.2222	0.1942	0.2016	0.2193	0.1942	0.2021

[#] Multiobjective particle swarm optimization.

Table A3
Generation Schedule (MW) and comparison for Test system-C.

Unit	No Loss			With Loss			OGHS [14]		
	MC	ME	CO	MC	ME	CO	MC	ME	CO
G1	55.00	55.00	37.38	55.00	55.00	55.00	55	55	55
G2	80.00	78.04	59.56	80.00	80.00	80.00	80	80	79.9998
G3	89.08	77.50	99.89	108.17	80.37	83.40	106.99	81.11	85.22
G4	80.20	77.50	109.78	100.06	80.37	81.57	100.54	81.41	84.30
G5	66.35	160.00	129.81	81.74	160.00	140.39	81.45	160.00	137.12
G6	70.00	240.00	215.79	82.09	240.00	158.89	83.07	240.00	155.89
G7	290.66	275.73	281.28	300.00	293.26	298.93	300.00	294.51	300.00
G8	328.72	277.73	301.51	340.00	295.84	315.39	340.00	297.26	315.73
G9	470.00	379.25	359.61	470.00	398.43	433.17	470.00	396.74	434.94
G10	470.00	379.25	405.38	470.00	398.43	437.46	470.00	395.57	436.01
Cost	106170.40	111867.55	110497.46	111497.95	116396.83	113278.18	111490.00	116410.00	113140.00
Emission	4278.76	3650.74	3880.03	4576.16	3932.42	4130.23	4572.27	3932.24	4144.41

Table A4
Generation Schedule (MW) and comparison for Test system-D.

Unit	No Loss			OGHS [14]			MABC# [14]		
	MC	ME	CO	MC	ME	CO	MC	ME	CO
G1	87.49	114.00	114.00	110.80	114.00	110.95	110.80	114.00	110.80
G2	73.40	114.00	114.00	110.80	114.00	111.02	110.80	114.00	110.80
G3	97.40	120.00	120.00	97.40	120.00	120.00	97.40	120.00	97.40
G4	179.73	169.37	179.73	179.73	169.41	179.73	179.73	169.37	174.55
G5	87.80	97.00	97.00	87.80	97.00	97.00	87.80	97.00	87.80
G6	139.99	124.26	137.14	140.00	124.22	140.00	140.00	124.26	105.40
G7	259.60	299.71	300.00	259.60	299.72	300.00	259.60	299.71	259.60
G8	284.60	297.91	300.00	284.60	297.98	284.60	284.60	297.91	284.60
G9	209.80	297.26	300.00	284.60	297.23	284.60	284.60	297.26	284.60
G10	279.60	130.00	130.00	130.00	130.00	130.00	130.00	130.00	130.00
G11	318.40	298.41	318.31	94.00	298.39	318.40	94.00	298.41	318.19
G12	243.60	298.03	317.68	94.00	298.04	318.40	94.00	298.03	243.60
G13	304.52	433.56	394.28	214.76	433.61	394.28	214.76	433.56	394.28
G14	394.28	421.73	394.28	394.28	421.74	394.28	394.28	421.73	394.28
G15	394.28	422.78	394.28	394.27	422.78	394.28	394.28	422.78	394.28
G16	394.28	422.78	394.28	394.28	422.69	394.28	394.28	422.78	394.28
G17	309.76	439.41	476.47	489.28	439.35	489.28	489.28	439.41	399.52
G18	489.28	439.40	476.55	489.28	439.28	489.28	489.28	439.40	399.52
G19	511.28	439.41	434.69	511.28	439.52	499.32	511.28	439.41	506.20
G20	511.28	439.41	434.52	511.28	439.45	421.52	511.28	439.41	506.18
G21	433.52	439.45	433.52	523.28	439.53	433.52	523.28	439.45	514.15
G22	523.28	439.45	436.15	523.28	439.46	433.52	523.28	439.45	514.15
G23	523.28	439.77	437.00	523.28	439.76	433.52	523.28	439.77	514.52
G24	523.28	439.77	436.95	523.28	439.76	433.52	523.28	439.77	514.54
G25	523.28	440.11	436.02	523.28	440.20	433.52	523.28	440.11	433.52
G26	523.28	440.11	435.75	523.28	440.21	433.52	523.28	440.11	433.52
G27	10.01	28.99	14.39	10.00	28.95	10.00	10.00	28.99	10.00
G28	10.01	28.99	14.38	10.00	29.09	10.00	10.00	28.99	10.00
G29	10.01	28.99	14.38	10.00	28.93	10.00	10.00	28.99	10.00
G30	87.80	97.00	97.00	87.80	97.00	97.00	87.80	97.00	97.00
G31	159.73	172.33	184.09	190.00	172.28	190.00	190.00	172.33	159.73
G32	189.99	172.33	184.09	190.00	172.27	190.00	190.00	172.33	159.73
G33	189.99	172.33	184.08	190.00	172.32	190.00	190.00	172.33	159.73
G34	90.02	200.00	200.00	164.80	200.00	200.00	164.80	200.00	200.00
G35	164.80	200.00	200.00	194.41	200.00	200.00	200.00	200.00	200.00
G36	199.94	200.00	200.00	200.00	200.00	200.00	194.40	200.00	200.00
G37	109.98	100.84	110.00	110.00	100.85	110.00	110.00	100.84	89.11
G38	89.11	100.84	110.00	110.00	100.81	89.13	110.00	100.84	89.11
G39	57.06	100.84	110.00	110.00	100.79	110.00	110.00	100.84	89.11
G40	511.28	439.41	434.98	511.28	439.38	421.52	511.28	439.41	506.19
Cost	124473.98	129954.64	126551.29	121403.60	129996.00	125346.70	121412.54	129995.27	124490.90
Emission	346740.38	176682.26	188453.68	359899.00	176681.40	202038.80	359901.47	176682.26	256560.26

Modified artificial bee colony optimization.

References

[1] United Nations Millennium Development Goals. [Online]. Available: http://www.un.org/millenniumgoals/environ.shtml.

[2] Clean Development Mechanism. United Nations Framework Convention on Climate Change. [Online]. Available: http://cdm.unfccc.int/.

[3] CDM Methodologies. [Online]. Available: http://cdm.unfccc.int/methodologies/index.html.

[4] CDM Registered Projects. Available Online: https://cdm.unfccc.int/Projects/registered.html.

[5] Denny E, O'Malley M. Wind generation, power system operation, and emissions reduction. IEEE Trans Power Syst 2006;21(1):341–7. https://doi.org/10.1109/TPWRS.2005.857845.

[6] Gil HA, Joos G. Generalized estimation of average displaced emissions by wind generation. IEEE Trans Power Syst 2007;22(3):1035–43. https://doi.org/10.1109/TPWRS.2007.901482.

[7] Abido MA. Multiobjective evolutionary algorithms for electric power dispatch problem. IEEE Trans Evol Comput 2006;10(3):315–29. https://doi.org/10.1109/TEVC.2005.857073.

[8] Abido MA. Multiobjective particle swarm optimization for environmental/economic dispatch problem. Electric Power Syst Res 0378-77962009;79(7):1105–13. https://doi.org/10.1016/j.epsr.2009.02.005.

[9] Basu M. Economic environmental dispatch using multi-objective differential evolution. Appl Soft Comput 1568-49462011;11(2):2845–53. https://doi.org/10.1016/j.asoc.2010.11.014.

[10] Jadoun Vinay Kumar, Gupta Nikhil, Niazi KR, Swarnkar Anil. Modulated particle swarm optimization for economic emission dispatch. Int J Electric Power Energy Syst 0142-06152015;73:80–8. https://doi.org/10.1016/j.ijepes.2015.04.004.

[11] Sen Tanuj, Mathur Hitesh Datt. A new approach to solve Economic Dispatch problem using a Hybrid ACO–ABC–HS optimization algorithm. Int J Electric Power Energy Syst 0142-06152016;78:735–44. https://doi.org/10.1016/j.ijepes.2015.11.121.

[12] Nguyen Thang Trung, Vo Dieu Ngoc, Dinh Bach Hoang. Cuckoo search algorithm for combined heat and power economic dispatch. Int J Electric Power Energy Syst 0142-06152016;81:204–14. https://doi.org/10.1016/j.ijepes.2016.02.026.

[13] Chen F, Huang GH, Fan YR, Liao RF. A nonlinear fractional programming approach for environmental–economic power dispatch. Int J Electric Power Energy Syst 0142-06152016;78:463–9. https://doi.org/10.1016/j.ijepes.2015.11.118.

[14] Singh Manmohan, Dhillon JS. Multiobjective thermal power dispatch using opposition-based greedy heuristic search. Int J Electric Power Energy Syst 0142-06152016;82:339–53. https://doi.org/10.1016/j.ijepes.2016.03.016.

[15] Rajan Abhishek, Malakar T. Optimum economic and emission dispatch using exchange market algorithm. Int J Electric Power Energy Syst 0142-06152016;82:545–60. https://doi.org/10.1016/j.ijepes.2016.04.022.

[16] Pan Shanshan, Jian Jinbao, Yang Linfeng. A hybrid MILP and IPM approach for dynamic economic dispatch with valve-point effects. Int J Electric Power Energy Syst 0142-06152018;97:290–8. https://doi.org/10.1016/j.ijepes.2017.11.004.

[17] Lokeshgupta B, Sivasubramani S. Multi-objective dynamic economic and emission dispatch with demand side management. Int J Electric Power Energy Syst 0142-06152018;97:334–43. https://doi.org/10.1016/j.ijepes.2017.11.020.

[18] Jabbari Ghadi M, Itami Karin A, Baghramian A, Hosseini Imani M. Optimal power scheduling of thermal units considering emission constraint for GENCOs profit maximization. Int J Electric Power Energy Syst 0142-06152016;82:124–35. https://doi.org/10.1016/j.ijepes.2016.03.011.

[19] Benidris Mohammed, Elsaiah Salem, Mitra Joydeep. An emission-constrained approach to power system expansion planning. Int J Electric Power Energy Syst 0142-

06152016;81:78–86. https://doi.org/10.1016/j.ijepes.2016.01.052.
[20] Hetzer J, Yu DC, Bhattarai K. An economic dispatch model incorporating wind power. IEEE Trans Energy Convers 2008;23(2):603–11. https://doi.org/10.1109/TEC.2007.914171.
[21] Liu X, Xu W. Economic load dispatch constrained by wind power availability: a here-and-now approach. IEEE Trans Sustain Energy 2010;1(1):2–9. https://doi.org/10.1109/TSTE.2010.2044817.
[22] Liu X. Economic load dispatch constrained by wind power availability: a wait-and-see approach. IEEE Trans Smart Grid 2010;1(3):347–55. https://doi.org/10.1109/TSG.2010.2057458.
[23] Liu X, Xu W. Minimum emission dispatch constrained by stochastic wind power availability and cost. IEEE Trans Power Syst 2010;25(3):1705–13. https://doi.org/10.1109/TPWRS.2010.2042085.
[24] Zhu Yongsheng, Wang Jie, Qu Boyang. Multi-objective economic emission dispatch considering wind power using evolutionary algorithm based on decomposition. Int J Electric Power Energy Syst 0142-06152014;63:434–45. https://doi.org/10.1016/j.ijepes.2014.06.027.
[25] Jiang Shanhe, Ji Zhicheng, Wang Yan. A novel gravitational acceleration enhanced particle swarm optimization algorithm for wind thermal economic emission dispatch problem considering wind power availability. Int J Electric Power Energy Syst 0142-06152015;73:1035–50. https://doi.org/10.1016/j.ijepes.2015.06.014.
[26] Pandit Manjaree, Chaudhary Vishal, Dubey Hari Mohan, Panigrahi BK. Multi-period wind integrated optimal dispatch using series PSO-DE with time-varying Gaussian membership function based fuzzy selection. Int J Electric Power Energy Syst 0142-06152015;73:259–72. https://doi.org/10.1016/j.ijepes.2015.05.017.
[27] Lau ET, Yang Q, Taylor GA, Forbes AB, Wright PS, Livina VN. Optimisation of costs and carbon savings in relation to the economic dispatch problem as associated with power system operation. Electric Power Syst Res 0378-77962016;140:173–83. https://doi.org/10.1016/j.epsr.2016.06.025.
[28] Lujano-Rojas JM, Osrio GJ, Catal JPS. New probabilistic method for solving economic dispatch and unit commitment problems incorporating uncertainty due to renewable energy integration. Int J Electric Power Energy Syst 0142-06152016;78:61–71. https://doi.org/10.1016/j.ijepes.2015.11.064.
[29] Banerjee Sumit, Dasgupta Koustav, Chanda Chandan Kumar. Short term hydro–-wind–thermal scheduling based on particle swarm optimization technique. Int J Electric Power Energy Syst 0142-06152016;81:275–88. https://doi.org/10.1016/j.ijepes.2016.01.031.
[30] Jangamshetti SH, Guruprasada Rau V. Normalized power curves as a tool for identification of optimum wind turbine generator parameters. IEEE Trans Energy Convers 2001;16(3):283–8. https://doi.org/10.1109/60.937209.
[31] Burton Tony, Sharpe David, Jenkins Nick, Bossanyi Ervin. Wind Energy Handbook. John Wiley & Sons Ltd.; 2001.
[32] Chandel SS, Ramasamy P, Murthy KSR. Wind power potential assessment of 12 locations in western Himalayan region of India. Renew Sustain Energy Rev 1364-03212014;39:530–45. https://doi.org/10.1016/j.rser.2014.07.050.
[33] Jiang He, Wang Jianzhou, Dong Yao, Lu Haiyan. Comprehensive assessment of wind resources and the low-carbon economy: an empirical study in the Alxa and Xilin Gol Leagues of inner Mongolia China. Renew Sustain Energy Rev 1364-03212015;50:1304–19. https://doi.org/10.1016/j.rser.2015.05.082.
[34] Ma XY, Sun YZ, Fang HL. Scenario generation of wind power based on statistical uncertainty and variability. IEEE Trans Sustain Energy 2013;4(4):894–904. https://doi.org/10.1109/TSTE.2013.2256807.
[35] Feijóo Andrés, Villanueva Daniel, Feijóo Andrés, Villanueva Daniel. Assessing wind speed simulation methods. Renew Sustain Energy Rev 1364-03212016;56:473–83. https://doi.org/10.1016/j.rser.2015.11.094.
[36] Gualtieri Giovanni, Secci Sauro. Methods to extrapolate wind resource to the turbine hub height based on power law: a 1-h wind speed vs. Weibull distribution extrapolation comparison. Renew Energy 0960-14812012;43:183–200. https://doi.org/10.1016/j.renene.2011.12.022.
[37] Thapar Vinay, Agnihotri Gayatri, Sethi Vinod Krishna. Critical analysis of methods for mathematical modelling of wind turbines. Renew Energy 0960-14812011;36(11):3166–77. https://doi.org/10.1016/j.renene.2011.03.016.
[38] Celik Ali Naci. Energy output estimation for small-scale wind power generators using Weibull-representative wind data. J Wind Eng Indus Aerodyn 0167-61052003;91(5):693–707. https://doi.org/10.1016/S0167-6105(02)00471-3.
[39] Tool to calculate emission factor for an electricity system. [Online]. Available: https://cdm.unfccc.int/methodologies/PAmethodologies/tools/am-tool-07-v5.0.pdf.
[40] Zamani Ali Ghahgharaee, Zakariazadeh Alireza, Jadid Shahram, Kazemi Ahad. Stochastic operational scheduling of distributed energy resources in a large scale virtual power plant. Int J Electric Power Energy Syst 0142-06152016;82:608–20. https://doi.org/10.1016/j.ijepes.2016.04.024.
[41] Xiao Qing. Comparing three methods for solving probabilistic optimal power flow. Electric Power Syst Res 0378-77962015;124:92–9. https://doi.org/10.1016/j.epsr.2015.03.001.